ALEPH 95-103
PHYSIC 95-92
A.M. Greene
18.8.1995

A Likelihood-Based Jet Charge Method

A M Greene, Institut für Physik, Universität Mainz

August 17, 1995

Abstract

The motivation behind the use of jet charges is discussed and existing jet charge methods are summarised. A new jet charge method based on a ratio of likelihoods is presented. The method prescribes weights for use in a jet charge calculation which are specific to the needs of a given analysis. Moreover, the weights may be calculated so as to desensitize the resulting jet charge to any undesired source of charged tracks, particularly sources of charged tracks which make undesirable contributions to the systematic error on a measurement.

The method is compared with existing methods in the context of the setting of a lower limit for the B_s^0-$\bar{B}_s^0$ mixing parameter x_s.

1 Introduction

Important tests of the Standard Model have been made at LEP I through measurements of forward-backward quark charge asymmetries and of B^0-$\bar{B}^0$ mixing. These measurements require, event by event, information about the particle/antiparticle state of the primary quarks in the jets.

In $b\bar{b}$ and $c\bar{c}$ events, the high mass of the primary quarks allows them kinematically, through their semileptonic decays, to produce a lepton with a relatively high transverse momentum with respect to a jet. Since a lepton produced in a semileptonic decay has the same sign charge as the decaying quark, and since the production rate of secondary $b\bar{b}$ and $c\bar{c}$ pairs is expected to be suppressed to at least $O(10^{-2})$ per event [1], identified leptons with high transverse momentum can be and have been used [2, 3, 4] to determine the particle/antiparticle state of the primary quarks.

However, a fundamental disadvantage of using the leptons from semileptonic decays is the statistical limitation coming from the b and c quark semileptonic branching ratios, which are $O(10\%)$ [5]. Since primary quark particle/antiparticle state information is not only given by semileptonic b and c quark decays, but also, according to the hadronization model [6], by the charges of *all* the particles in the jet containing the quark, it is natural to look for a way of combining all those charges into one charge estimator, namely a "jet charge". Such an estimator does not rely on a semileptonic decay and is therefore not affected by any semileptonic branching ratio.

A jet charge Q is defined as the weighted sum of the charges q_i of the tracks in that jet or hemisphere,

$$Q = \sum_i w_i q_i, \qquad \text{Form (1)}$$

or the similarly weighted mean

$$Q = \frac{\sum_i w_i q_i}{\sum_i |w_i|}, \qquad \text{Form (2)}$$

where the weights w_i are chosen as a function of other properties of the tracks, normally empirically and as an increasing function of momentum. The motivation for this choice is the hadronization model [6], in which the faster tracks in a jet are more likely than the slower tracks to have the same sign charge as the primary quark in the jet. Figure 1 illustrates how the charge of a primary quark in the model propagates to the lowest rank charged particle even when the lowest rank hadron is neutral. Weights which are an increasing function of momentum

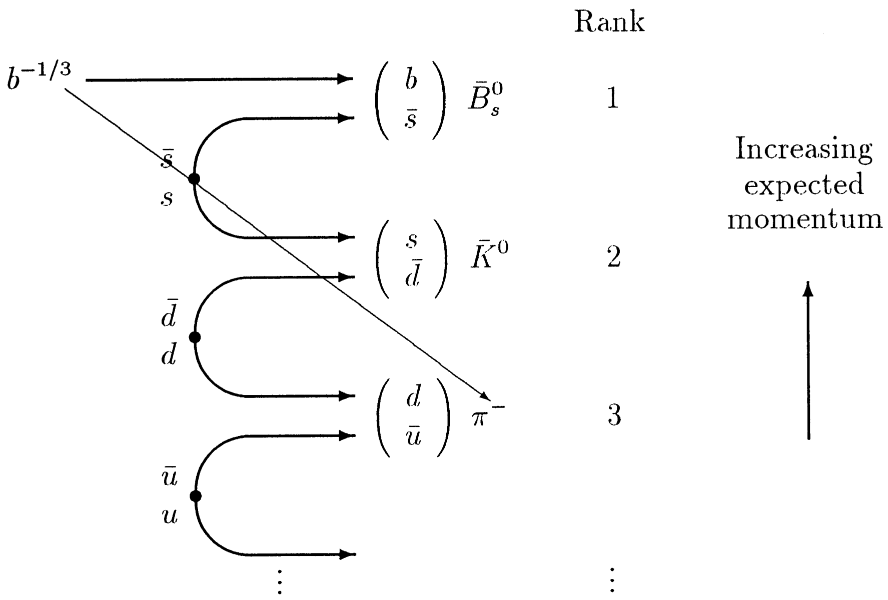

Figure 1: Propagation of the negative charge of a primary quark ($b^{-1/3}$) in the hadronization model [6] to the lowest rank charged hadron (π^-), in the case where the lowest rank hadron ($\bar{B}_s^0$) is neutral.

give the largest expected weight to the lowest rank hadron, resulting in the largest expected contribution to the jet charge coming from the lowest rank charged hadron, which holds the charge of the primary quark.

It is usual to cut on $|Q|$ and take the sign of Q as the charge. Jet charge was originally suggested in the form (1) [6], but forms (1) [11, 12] and (2) [7, 8, 9, 13, 14] have both been used successfully at LEP I. Examples of weight functions that have been suggested and/or used are

$$\left.\begin{aligned} w_i &= \left[\frac{E_i + p_{\parallel i}}{E_0 + p_{\parallel 0}}\right]^\kappa && [6] \\ &= \left(\frac{p_{\parallel i}}{E_b}\right)^\kappa && [11,\ 12] \\ &= 1 && [11,\ 12] \end{aligned}\right\}\ \text{Form (1)}$$

$$\left.\begin{aligned} &= {p_{\parallel i}}^\kappa && [7,\ 8,\ 9,\ 13,\ 14] \\ &= 1 && \\ &= y_i = \frac{1}{2}\ln\frac{E_i + p_{\parallel i}}{E_i - p_{\parallel i}} && [10] \\ &= p_{\perp i}, && \end{aligned}\right\}\ \text{Form (2)} \qquad (3)$$

where E_i is the energy of track i whose longitudinal and transverse 3-momentum components $p_{\parallel i}$ and $p_{\perp i}$ are measured with respect to the thrust, sphericity or jet axis, and where E_b denotes the beam energy (approx. 46 GeV at LEP I), $i = 0$ denotes the primary quark in the jet and κ is a parameter varied to optimize the jet charge performance.

2 A Likelihood-Based Jet Charge Method

One disadvantage of using the empirical jet charge weight functions in (3) is the uncertainty about which functions are suitable for a particular analysis. This uncertainty is avoided by a likelihood-based jet charge method, where a unique weight function can be created in order to satisfy the specific needs of a given analysis.

As an example, consider a jet charge weight function $w_i = w_i(p_{\parallel i}, p_{\perp i})$ and the schematic view of the ($p_\parallel$,$p_\perp$) distribution in an event hemisphere shown in Figure 2. The function $x(p_\parallel, p_\perp)$ is defined as the probability that a track with parallel and transverse momentum components $p_\parallel$ and $p_\perp$, which is selected at random from the set of all good tracks in $Z \to b\bar{b}$ event hemispheres, has the same sign charge as the b or $\bar{b}$ quark in that same hemisphere. Using this function together with the assumption of the statistical independence of tracks, it is possible, with a hemisphere such as in Figure 2, to calculate the likelihoods for the different hypotheses of $\bar{b}$ and b as simple products. Writing $x(p_{\parallel i}, p_{\perp i})$ as x_i, with the charge configuration in Figure 2 the respective likelihoods L_+ and L_- for the $\bar{b}$ and b hypotheses become

$$L_+ = (1 - x_1)x_2x_3(1 - x_4)x_5 \qquad (4)$$
$$L_- = x_1(1 - x_2)(1 - x_3)x_4(1 - x_5). \qquad (5)$$

The ratio of the likelihoods is then

$$\frac{L_+}{L_-} = \prod_i \left[\frac{x_i}{1 - x_i}\right]^{q_i} = \prod_i {r_i}^{q_i}, \qquad (6)$$

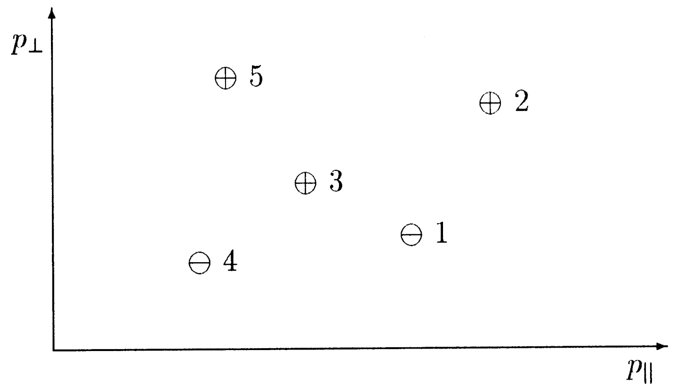

Figure 2: Schematic view of the ($p_\parallel$,$p_\perp$) distribution in an event hemisphere containing 5 tracks with positive (⊕) and negative (⊖) charges.

where q_i is the charge of track i and $r_i = x_i/(1 - x_i)$. The logarithm of this ratio

$$\log\left(\frac{L_+}{L_-}\right) = \sum_i q_i \log r_i \tag{7}$$

preserves ordering by jet charge, since $a > b$ implies $\log(a) > \log(b)$, and is simply a jet charge of the form (1).

Here $w_i = w_i(p_{\parallel i}, p_{\perp i}) = \log r_i$, but clearly w_i can be made a function of any set of parameters which is thought to be important. The function x, or equivalently r, can be determined from Monte Carlo. The method can be desensitized to any undesired source of charged tracks by creating the weight function for a special Monte Carlo sample, in which, at each occurrence of the undesired source, the particle/antiparticle state of the source has been randomized, with equal probabilities for particle and antiparticle.

As an example, the method is compared here with existing jet charge methods in the context of the setting of a lower limit for the B_s^0-$\bar{B}_s^0$ mixing parameter x_s. For this study, it was decided, in addition to $p_\parallel$ and $p_\perp$, to make use of the three-dimensional impact parameter d_{min} [16] of the tracks, so that $w_i = w_i(p_{\parallel i}, p_{\perp i}, d^i_{\text{min}})$.

3 A Comparison with Existing Jet Charge Methods in an Analysis Example

In principle at least, with the jet charge methods as described, the harder the cut on $|Q|$, the greater the probability of Q having the same sign as the charge of the primary quark in the hemisphere. The choice of methods, together with this trade-off between efficiency and probability, results in different analyses producing optimal results with different methods and with different cuts. That is to say, there is no universally "best" jet charge: the jet charge used in an analysis should depend on the details of that analysis.

The jet charge methods are compared here in the context of the setting of a lower limit for the B_s^0-$\bar{B}_s^0$ mixing parameter x_s, where an enriched sample of B_s^0 events with known final B_s^0 particle/antiparticle state was selected by reconstructing $D_s^\pm$ in the "$\phi\pi$" decay channel shown in Figure 3, and where the initial B_s^0 particle/antiparticle state was determined using a linear combination

$$Q_{AB} = c_A Q_A - c_B Q_B \tag{8}$$

of the jet charges Q_A and Q_B of the hemispheres. A schematic view of this analysis is shown in Figure 4. The coefficients c_A and c_B were calculated for optimal performance of Q_{AB}.

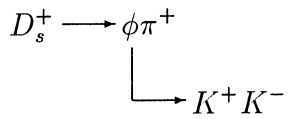

Figure 3: The "$\phi\pi$" decay channel.

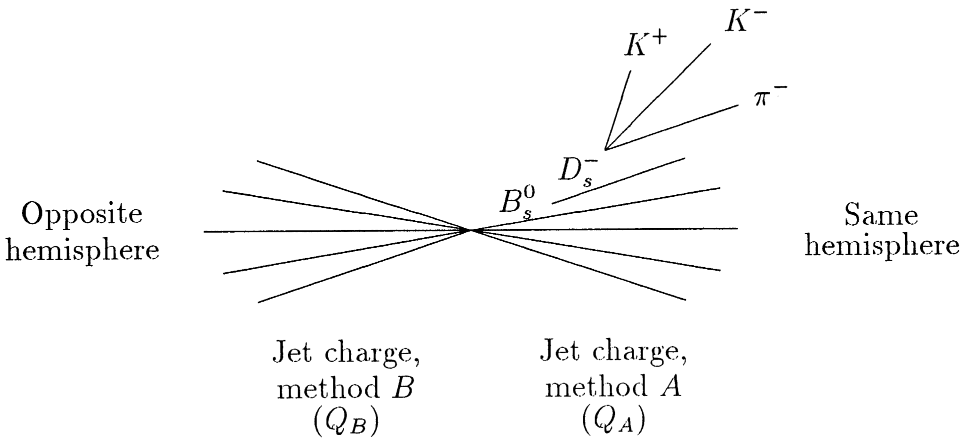

Figure 4: Schematic view of the analysis in the context of which the jet charge methods are compared. The final B_s^0 particle/antiparticle state was determined by the $D_s^\pm$ charge and the initial B_s^0 particle/antiparticle state was determined using the linear combination of jet charges $Q_{AB} = c_A Q_A - c_B Q_B$, where c_A and c_B were coefficients calculated for optimal performance of Q_{AB}.

For the purposes of comparing the jet charge methods, it is assumed that $B_s^0/\bar{B}_s^0$ has been correctly identified through the reconstruction of $D_s^\pm$, from which its final particle/antiparticle state is known, leaving its initial particle/antiparticle state to be determined with a jet charge method in just one hemisphere. Since the hemispheres are essentially independent, the "best" jet charge method can be determined separately for the same and opposite hemispheres and later combined to form Q_{AB}.

A lifetime independent measurement[1] of x_s is made by measuring the quantity

$$R = \frac{N(\text{mixed } B_s^0 \text{ decays})}{N(\text{unmixed } B_s^0 \text{ decays}) + N(\text{mixed } B_s^0 \text{ decays})}, \tag{9}$$

[1] Although, through lack of statistics, such an analysis could only realistically be expected to set a limit for x_s, it is easier to compare jet charge methods in the context of a measurement of x_s where the errors on x_s can be calculated and compared. Provided the "best" jet charge method and cut so determined are independent of the statistics of the data sample, it is reasonable to assume that by having minimised the error on x_s with hypothetical high statistics, one has maximised a limit set for x_s with the real, low statistics.

which is given in terms of x_s by

$$R = \frac{1}{2} \cdot \frac{x_s^2}{x_s^2 + 1}. \tag{10}$$

For the jet charge Q ($= Q_A$ or Q_B), as one varies the cut on $|Q|$, the probability p that Q has the same sign as the charge of the b or $\bar{b}$ quark in the hemisphere varies in the range $0.5 \leq p < 1$ so that one in fact measures a value

$$R_{\text{meas}} = R \cdot (2p - 1) + 1 - p. \tag{11}$$

In the analysis described, the calculation of the jet charge Q_A for the B_s^0 hemispheres includes tracks from the B_s^0 decay, making it likely in this case for the probability p to depend on whether the $B_s^0/\bar{B}_s^0$ underwent a mixed or an unmixed decay. Writing p_{mix} and $p_{\text{no mix}}$ for these probabilities, (11) becomes

$$R_{\text{meas}} = R \cdot (p_{\text{mix}} + p_{\text{no mix}} - 1) + 1 - p_{\text{no mix}}, \tag{12}$$

which, with the redefinition

$$p = (p_{\text{mix}} + p_{\text{no mix}})/2, \tag{13}$$

can be written as

$$R_{\text{meas}} = R \cdot (2p - 1) + 1 - p_{\text{no mix}}. \tag{14}$$

Here, the B_s^0 decay is an undesirable source of charged tracks because these tracks contaminate a jet charge which is being used to determine the *initial* $B_s^0/\bar{B}_s^0$ particle/antiparticle state, and because they introduce the systematic uncertainty of B decay model dependence. Thus it is advantageous to desensitize the jet charge Q_A to tracks from the B_s^0 decay according to the procedure described in Section 2, which moves Q_A towards $p_{\text{mix}} = p_{\text{no mix}}$.

The cut on $|Q|$ also has an efficiency ϵ, so that the statistical error δR_{meas} on R_{meas} varies as $1/\sqrt{\epsilon N}$, where N is the original number of B_s^0 with known final particle/antiparticle state. Propagating δR_{meas} through to δR in (11) or in (14) leads to

$$\delta R = \left| \frac{\partial R}{\partial R_{\text{meas}}} \right| \cdot \delta R_{\text{meas}} \tag{15}$$

$$\propto \frac{1}{|2p - 1|} \cdot \frac{1}{\sqrt{\epsilon}}, \tag{16}$$

from which, as suggested in [15], one can define a quality factor $\zeta \propto 1/\delta R$ as

$$\zeta = |2p - 1|\sqrt{\epsilon}. \tag{17}$$

4 The likelihood jet charge method in the B_s^0-$\bar{B}_s^0$ mixing analysis

For the B_s^0-$\bar{B}_s^0$ mixing analysis described in Section 3, weight functions $w(p_{\parallel}, p_{\perp}, d_{\text{min}})$ were calculated separately from Monte Carlo for the different analysis situations in the two hemispheres. The longitudinal and transverse 3-momentum components $p_{\parallel}$ and $p_{\perp}$ for each track were measured with respect to the closest jet to the track. The jets were determined by applying the JADE scaled invariant mass squared algorithm to the energy flow objects, using $Y_{\text{cut}} = 0.02$. Instead of the three-dimensional impact parameter d_{min}, the related `QIPBTAG` track probability

$\mathcal{P}_T$ was used [16]. The $(p_{\|}, p_{\perp})$ and $\mathcal{P}_T$ distributions of reconstructed tracks in Monte Carlo $b\bar{b}$ events[2] which pass the 'Class 16' track selection cuts [17] are shown in Figure 5.

In order to calculate the weight functions $w(p_{\|}, p_{\perp}, \mathcal{P}_T)$, reconstructed tracks in the Monte Carlo $b\bar{b}$ events which passed the Class 16 track selection cuts [17] were binned separately in $(p_{\|}, p_{\perp}, \mathcal{P}_T)$, according to whether the tracks had the same or the opposite sign charge as the b or $\bar{b}$ quark in the hemisphere. Three-dimensional binning was achieved with several two dimensional $(p_{\|}, p_{\perp})$ histograms, one for each $\log_{10}(\mathcal{P}_T)$ bin. The $(p_{\|}, p_{\perp})$ histograms and $\log_{10}(\mathcal{P}_T)$ binning were as in Figure 5.

The weight w was then calculated for each $(p_{\|}, p_{\perp}, \mathcal{P}_T)$ bin as

$$w = \log(n_{\rm s}/n_{\rm o}), \tag{18}$$

where $n_{\rm s}$ and $n_{\rm o}$ were the numbers of tracks in the bin which had respectively the same and the opposite sign charge as the b or $\bar{b}$ quark in the hemisphere. The weight functions were smoothed by replacing the value of w in each bin by the arithmetic mean of the nine values of w centred on that bin in the relevant $(p_{\|}, p_{\perp})$ histogram. To limit statistical fluctuations that would inhibit understanding of the weight functions, it was then required that

$$n_{\rm s} + n_{\rm o} \geq n_{\rm min}, \tag{19}$$

for some $n_{\rm min}$. In regions where (19) was not satisfied, w was set to zero.

The weight function $w(p_{\|}, p_{\perp}, \mathcal{P}_T)$ for the opposite hemisphere is shown in Figure 6 in selected $\mathcal{P}_T$ slices. The value $n_{\rm min} = 400$ was used. In all $\mathcal{P}_T$ ranges, large values of w occur for large $p_{\|}$ and $p_{\perp}$, where the decay products of the b-hadron are expected to lie. The weight function is smooth and bounded just as it is with existing jet charge methods, creating no special systematic problems.

The weight function $w(p_{\|}, p_{\perp}, \mathcal{P}_T)$ was calculated for the same hemisphere using Monte Carlo $b\bar{b}$ hemispheres[3] in which B_s^0 decayed to D_s^- or $\bar{B}_s^0$ decayed to D_s^+ and in which the $D_s^\pm$ was correctly reconstructed in the $\phi\pi$ decay channel. The systematically advantageous desensitization procedure described in Section 2 was applied to the tracks in the same hemisphere originating from the B_s^0 decay, moving the jet charge Q_A towards $p_{\rm mix} = p_{\rm no\ mix}$.

When the same hemisphere contains B_s^0 which does not undergo a mixed decay, the jet charge Q_A can be expressed as the sum

$$Q_A = Q_1 + Q_2 \tag{20}$$

of the two components

$$\begin{aligned} Q_1 &= \sum_{\substack{\text{non-}b\text{-tracks} \\ B_s^0 \text{ no mix}}} w_i q_i \\ Q_2 &= \sum_{\substack{b\text{-tracks} \\ B_s^0 \text{ no mix}}} w_i q_i, \end{aligned} \tag{21}$$

where the b-tracks are defined to be the tracks originating from the B_s^0 decay. The distributions of Q_1, Q_2 and (Q_1, Q_2) are shown in Figure 7 and can be seen to be well approximated by Gaussian distributions. Henceforth Q_1 and Q_2 will be used to denote a pair of (correlated)

[2] A sample of 170 000 Monte Carlo $Z \to b\bar{b}$ events was used, generated by HVFLO3/DYMU02/PHOTOS and processed by GALEPH 255, JULIA 271.08 and MINI 9.0

[3] A special sample of 50 000 Monte Carlo $Z \to q\bar{q}$ events was used, generated such that the $\phi\pi$ decay sequence shown in Figure 3 occurred at least once per event.

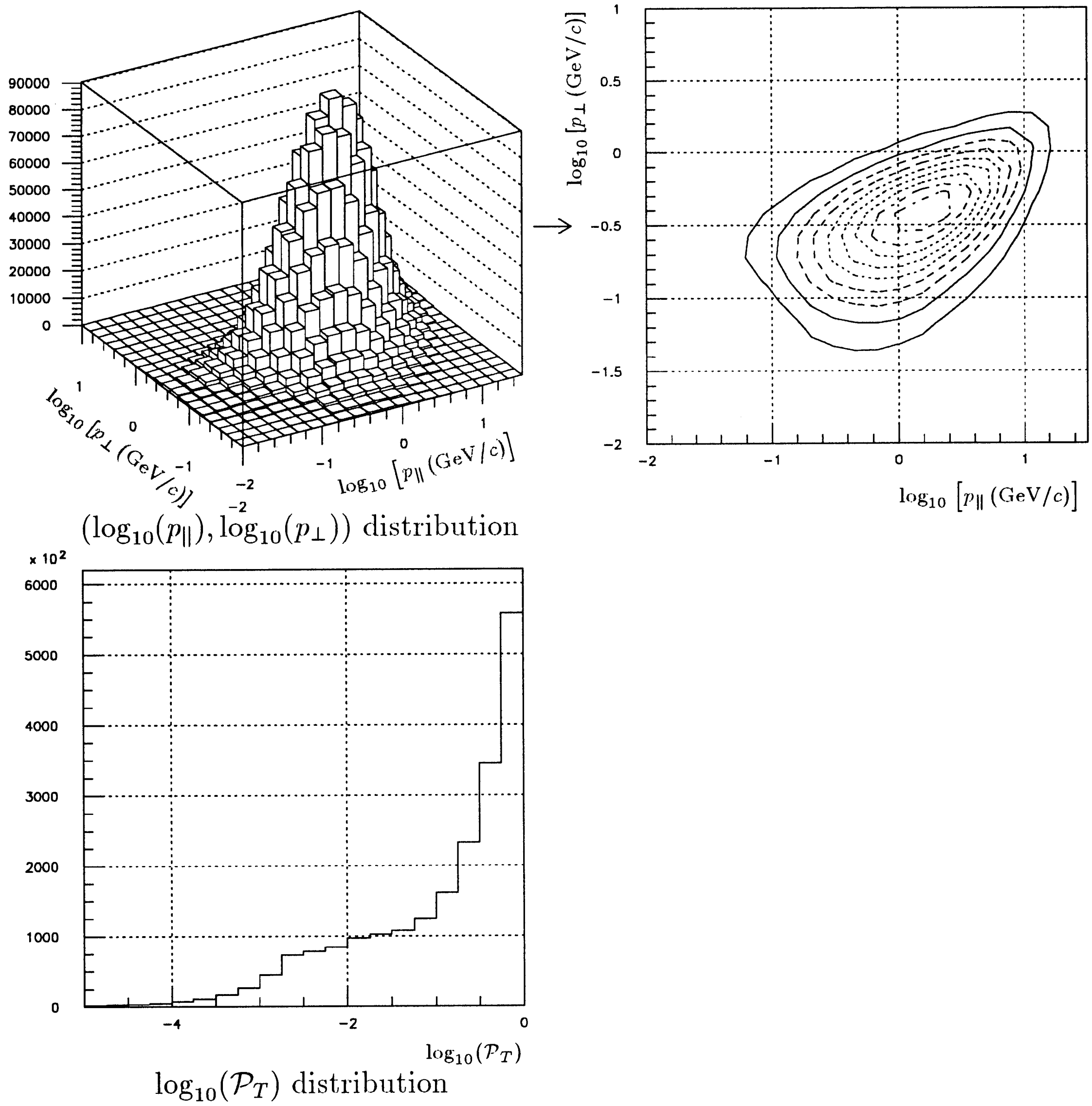

Figure 5: Distributions of the longitudinal and transverse momentum components $(p_\parallel, p_\perp)$ and the QIPBTAG track probabilities $\mathcal{P}_T$ of tracks in Monte Carlo $b\bar{b}$ events which pass the 'Class 16' track selection cuts [17].

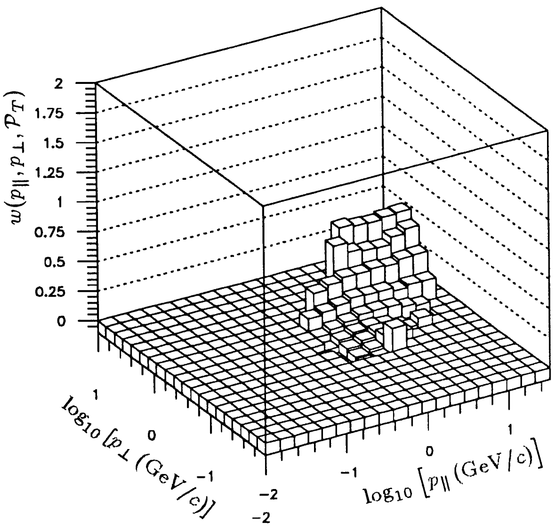

$-3.50 \leq \log_{10}(\mathcal{P}_T) < -3.25$

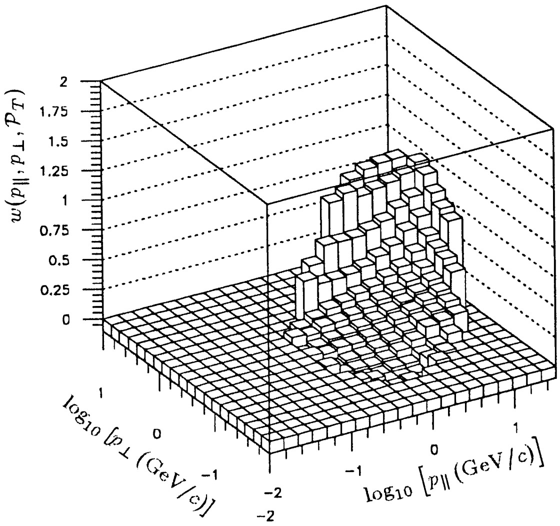

$-2.00 \leq \log_{10}(\mathcal{P}_T) < -1.75$

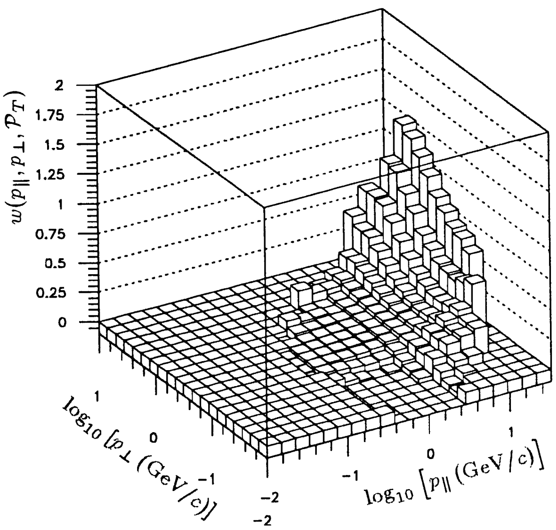

$-0.25 \leq \log_{10}(\mathcal{P}_T) \leq 0.00$

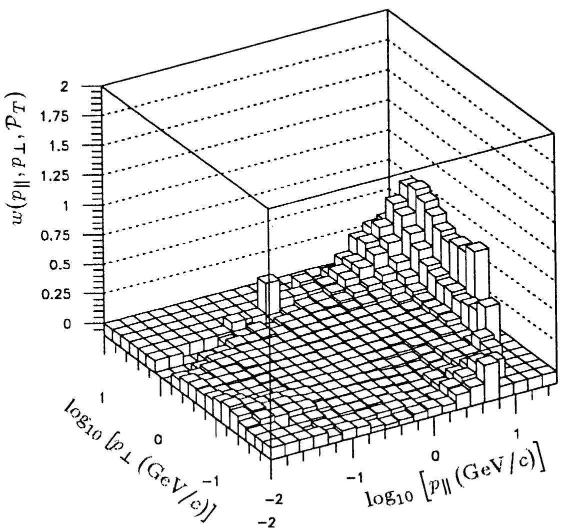

Tracks which pass the 'Class 16' track selection cuts [17], but which fail the `QIPBTAG` track selection cuts [16].

Figure 6: The weight function $w(p_{\|}, p_{\perp}, \mathcal{P}_T)$ for the opposite hemisphere.

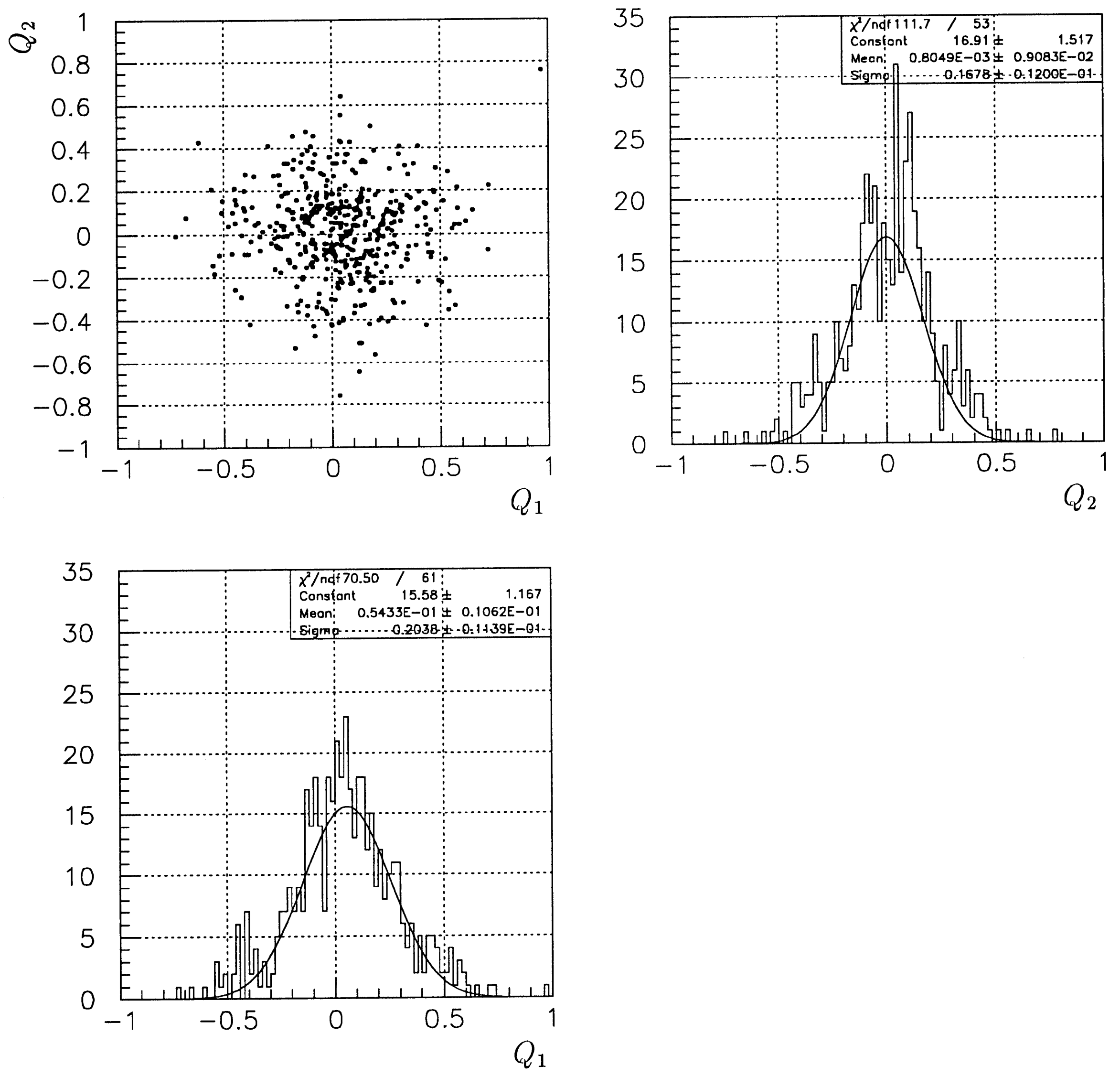

Figure 7: Q_1, Q_2 and (Q_1, Q_2) distributions and the results of fits to Gaussian distributions.

random variables sampled from the (Q_1, Q_2) distribution. The observed value of Q_A for the same hemisphere then depends on whether the B_s^0 underwent a mixed or an unmixed decay as follows:

$$Q_A = \begin{cases} Q_1 + Q_2 & (B_s^0 \text{ no mix}) \\ Q_1 - Q_2 & (B_s^0 \text{ mix}). \end{cases} \tag{22}$$

The crucial mean probability $(p_{\text{mix}} + p_{\text{no mix}})/2$ can then be calculated by artificially imposing a mixing probability χ_s of 1/2, whereby $Q_A = Q_1 \pm Q_2$, with equal probabilities for $Q_1 + Q_2$ and $Q_1 - Q_2$. In this situation, the mean and variance of Q_A

$$\begin{aligned} \mu_A &= \langle Q_A \rangle \\ \sigma_A^2 &= \langle (Q_A - \mu_A)^2 \rangle \end{aligned} \tag{23}$$

can be expressed in terms of the means and variances of Q_1 and Q_2

$$\begin{aligned} \mu_1 &= \langle Q_1 \rangle \\ \sigma_1^2 &= \langle (Q_1 - \mu_1)^2 \rangle \\ \mu_2 &= \langle Q_2 \rangle \\ \sigma_2^2 &= \langle (Q_2 - \mu_2)^2 \rangle, \end{aligned} \tag{24}$$

independently from the covariance $\langle (Q_1 - \mu_1)(Q_2 - \mu_2) \rangle$, as

$$\begin{aligned} \mu_A &= \mu_1 \\ \sigma_A^2 &= \sigma_1^2 + \sigma_2^2 + \mu_2^2. \end{aligned} \tag{25}$$

Thus in the Gaussian approximation, μ_A/σ_A, the significance of the jet charge Q_A in hemispheres containing B_s^0 or $\bar{B}_s^0$ with $\chi_s = 1/2$, is given by

$$\frac{\mu_A}{\sigma_A} = \frac{\mu_1}{\sqrt{\sigma_1^2 + \sigma_2^2 + \mu_2^2}}. \tag{26}$$

The desensitization procedure described in Section 2, when applied to the tracks in the same hemisphere originating from the B_s^0 decay, moves the jet charge Q_A towards $p_{\text{mix}} = p_{\text{no mix}}$. However, (26) shows that this does not guarantee an increase in the mean probability $(p_{\text{mix}} + p_{\text{no mix}})/2$. For example, $\mu_2 = 0$ ensures $p_{\text{mix}} = p_{\text{no mix}}$, but there is no upper limit on $\sigma_1^2 + \sigma_2^2$ in (26) and hence no limit on how small the significance μ_A/σ_A may be.

Fortunately, in practice μ_A/σ_A did increase with the desensitization of Q_A. The resulting weight function for the same hemisphere is shown in Figure 8 in selected $\mathcal{P}_T$ slices. The value $n_{\text{min}} = 100$ was used. Large values of w occur where $\log_{10}(\mathcal{P}_T)$ is close to 0, corresponding to tracks which are consistent with having come from the interaction point and not from the decay of a long-lived b-hadron. These tracks are likely to have rank 2 or above as defined in Figure 1, where the charge information is independent of the final particle/antiparticle state of the B_s^0.

The effect of the desensitization procedure is shown in Figure 9, and the sensitivities of existing jet charge methods are shown in Figure 10 for comparison. Only the desensitized likelihood jet charge and $Q_A = \sum_i q_i/N$ are consistent with being insensitive to whether the $B_s^0/\bar{B}_s^0$ underwent a mixed or an unmixed decay.

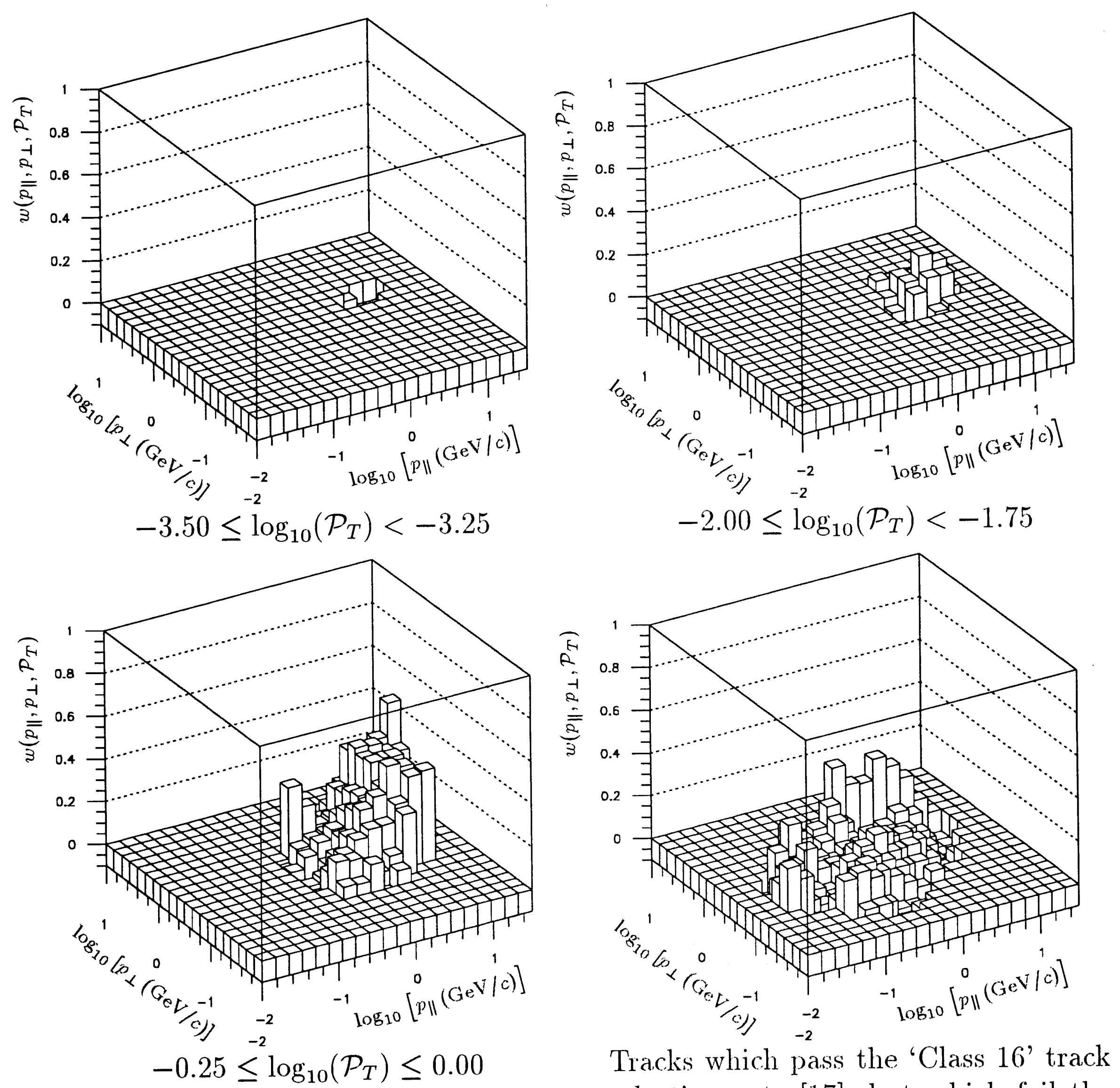

Tracks which pass the 'Class 16' track selection cuts [17], but which fail the QIPBTAG track selection cuts [16].

Figure 8: The desensitized weight function $w(p_{\parallel}, p_{\perp}, \mathcal{P}_T)$ for the same hemisphere.

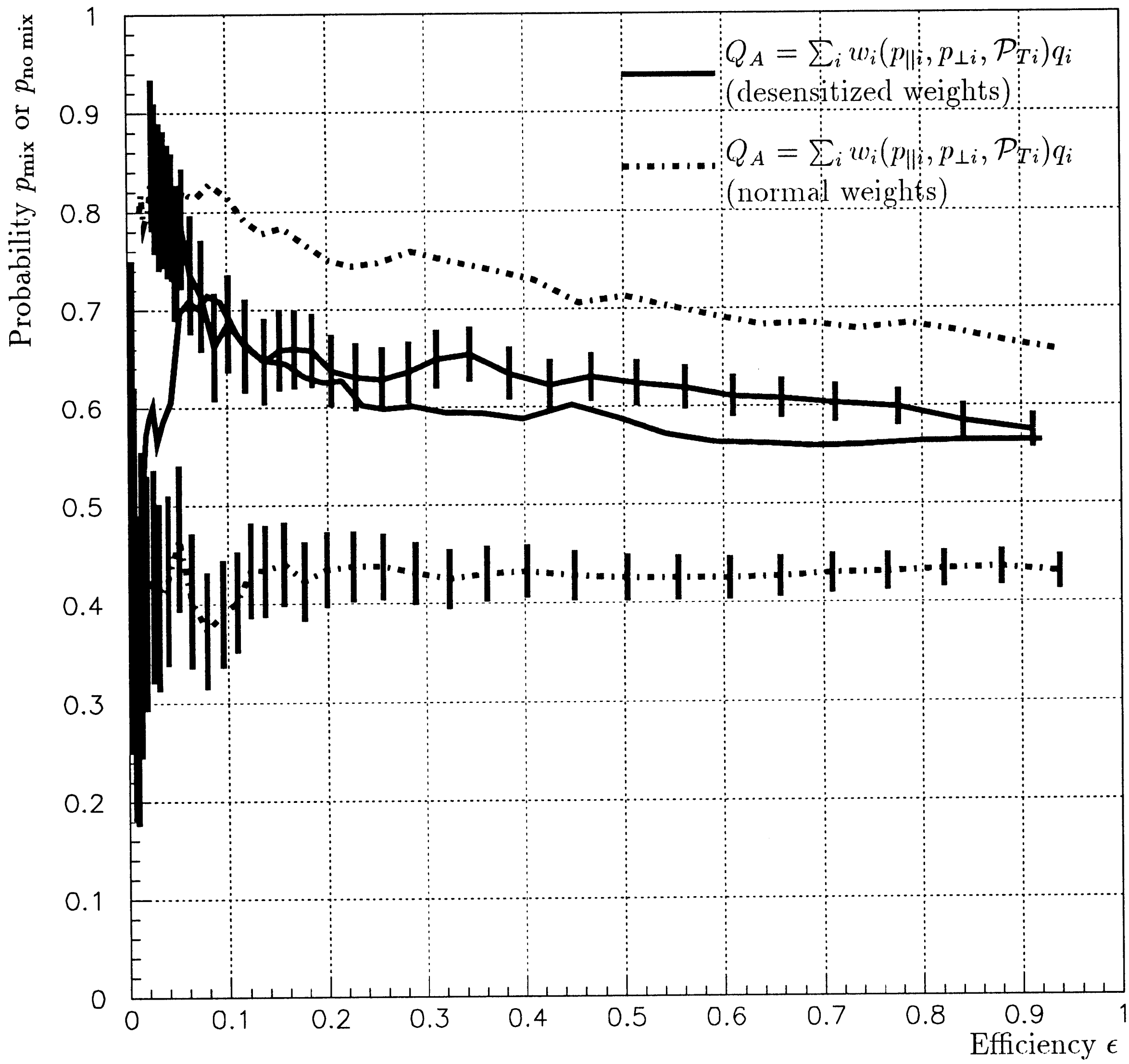

Figure 9: The effect of the procedure to desensitize the likelihood jet charge Q_A in the same hemisphere to the tracks originating from the B_s^0 decay. The curves show the variation of p with the efficiency ϵ of the cut on $|Q_A|$, for the cases of the $B_s^0/\bar{B}_s^0$ undergoing a mixed or unmixed decay, with the standard or desensitized weights. Error bars are only shown for the cases of the $B_s^0/\bar{B}_s^0$ undergoing an unmixed decay, and since a cut is being varied, these errors are correlated. The normal weights are shown in Figure 6 and the desensitized weights are shown in Figure 8. In order to simulate the situation in the same hemisphere, only those Monte Carlo $Z \to b\bar{b}$ hemispheres were used in which B_s^0 decayed to D_s^- or $\bar{B}_s^0$ decayed to D_s^+, and in which the $D_s^\pm$ was correctly reconstructed in the $\phi\pi$ decay channel.

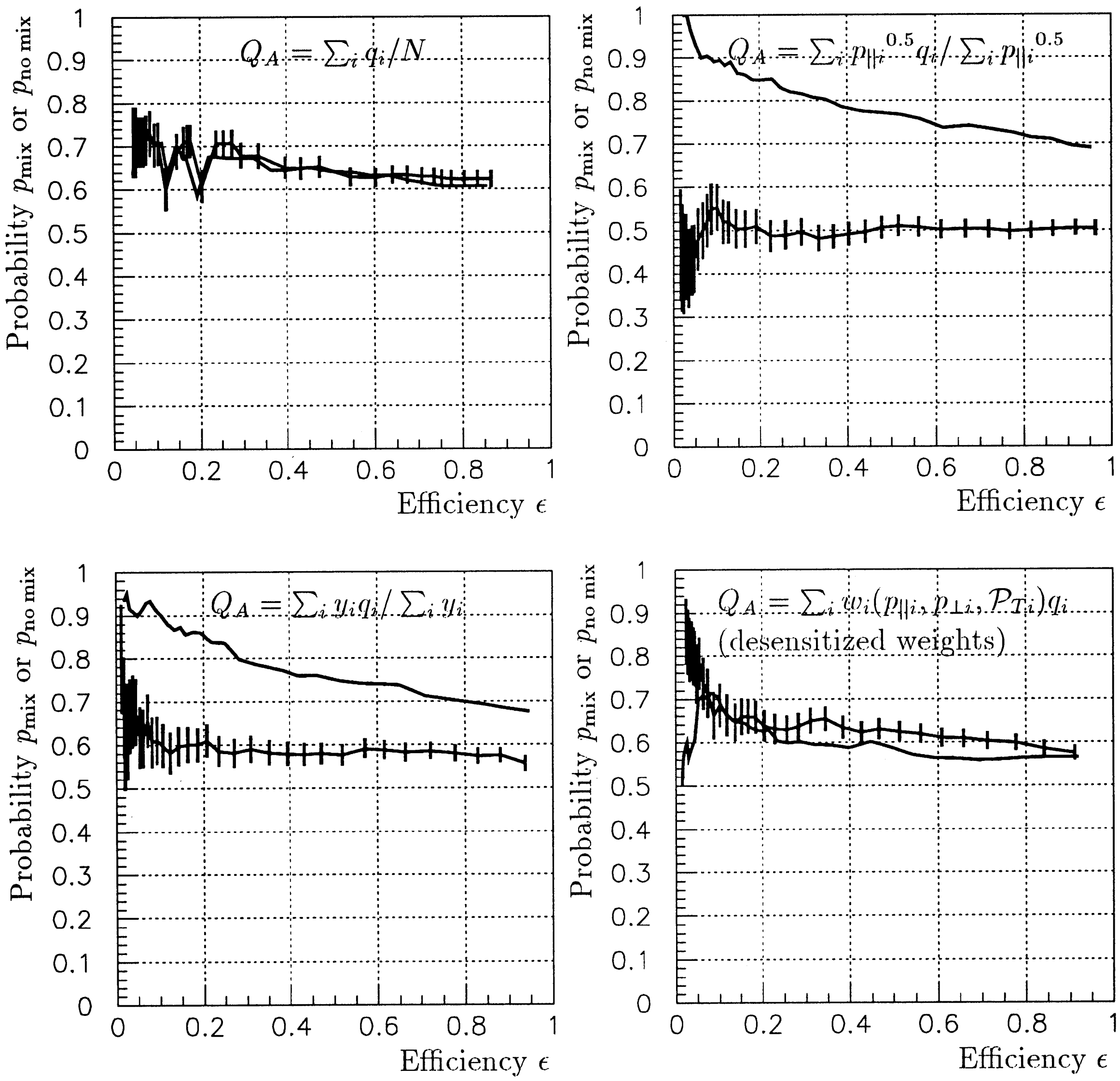

Figure 10: The sensitivity of existing jet charge methods in the same hemisphere to whether the $B_s^0/\bar{B}_s^0$ underwent a mixed or an unmixed decay. Comments as for Figure 9.

5 Results of the Comparison with Existing Jet Charge Methods

The variations of p with the efficiency ϵ of the cut on $|Q|$ for different jet charge methods in the opposite and same hemispheres are shown in Figures 11 and 12, with contours of the quality factor ζ. For the jet charge methods $Q = \sum_i p_{\parallel i}{}^{\kappa} q_i / \sum_i p_{\parallel i}{}^{\kappa}$ and $Q = \sum_i (p_{\parallel i}/E_b)^{\kappa} q_i$, the parameter κ was varied and the optimal value was found to be $\kappa \simeq 0.5$ for the opposite hemisphere and $\kappa \simeq 0$ for the same hemisphere. Hence, these values of κ are featured in the plots.

Figure 11 shows that there is indeed something to be gained in the opposite hemisphere by using jet charge instead of leptons — even though jet charges are less likely to give the correct charge, this is more than offset by their statistical advantage. Also, the likelihood jet charge method does not perform as well as the tried and tested method $Q = \sum_i p_{\parallel i}{}^{0.5} q_i / \sum_i p_{\parallel i}{}^{0.5}$ [7, 8, 13]. Furthermore, with $w_i = p_{\parallel i}{}^{0.5}$, the form (1) performs slightly better than the form (2) used by ALEPH [7, 8].

Figure 12 shows that the desensitized likelihood jet charge does indeed perform better than the standard likelihood jet charge. It has comparable performance to the method $Q_A = \sum_i q_i/N$, the only existing method which also is insensitive to whether the $B_s^0/\bar{B}_s^0$ underwent a mixed or an unmixed decay.

6 A Comparison Between Data and Monte Carlo

The Monte Carlo simulation of the efficiencies and probabilities of jet charge methods depends both on the hadronization model used and the values of the parameters in the model. Although the model and the parameters are "tuned" to the data on a global basis, in specific instances there could still be significant discrepancies between data and Monte Carlo. Therefore, ideally, one should measure the efficiencies and probabilities directly from the data. However, it is not possible to measure ϵ and p directly since this would at least require a pure sample of event hemispheres in which B_s^0 decayed to D_s^- or $\bar{B}_s^0$ decayed to D_s^+ which is not available. Instead one must make do with more inclusive measurements of ϵ and p which include backgrounds but which nevertheless can be used for a representative comparison between data and Monte Carlo.

To this end, unbinned log-likelihood fits were made to the (Q_A, Q_B) jet charge distributions, using the function

$$f(Q_A, Q_B) = \frac{1}{2\pi\sigma_A\sigma_B}\left(\exp\left[-\frac{(Q_A-\mu_A)^2}{2\sigma_A^2} - \frac{(Q_B+\mu_B)^2}{2\sigma_B^2}\right] + \exp\left[-\frac{(Q_A+\mu_A)^2}{2\sigma_A^2} - \frac{(Q_B-\mu_B)^2}{2\sigma_B^2}\right]\right) \quad (27)$$

and allowing the parameters μ_A, σ_A, μ_B and σ_B to vary. The function reflects the expected distribution of (Q_A, Q_B), that is, two Gaussian distributions, one centred at $(\mu_A, -\mu_B)$ corresponding to events where the same hemisphere contained $\bar{b}$, and the other centred at $(-\mu_A, \mu_B)$ corresponding to events where the same hemisphere contained b.

The fits were performed for the likelihood jet charge set up as described for the B_s^0-$\bar{B}_s^0$ mixing analysis, using events in which a $D_s^{\pm}$ candidate was reconstructed within the mass

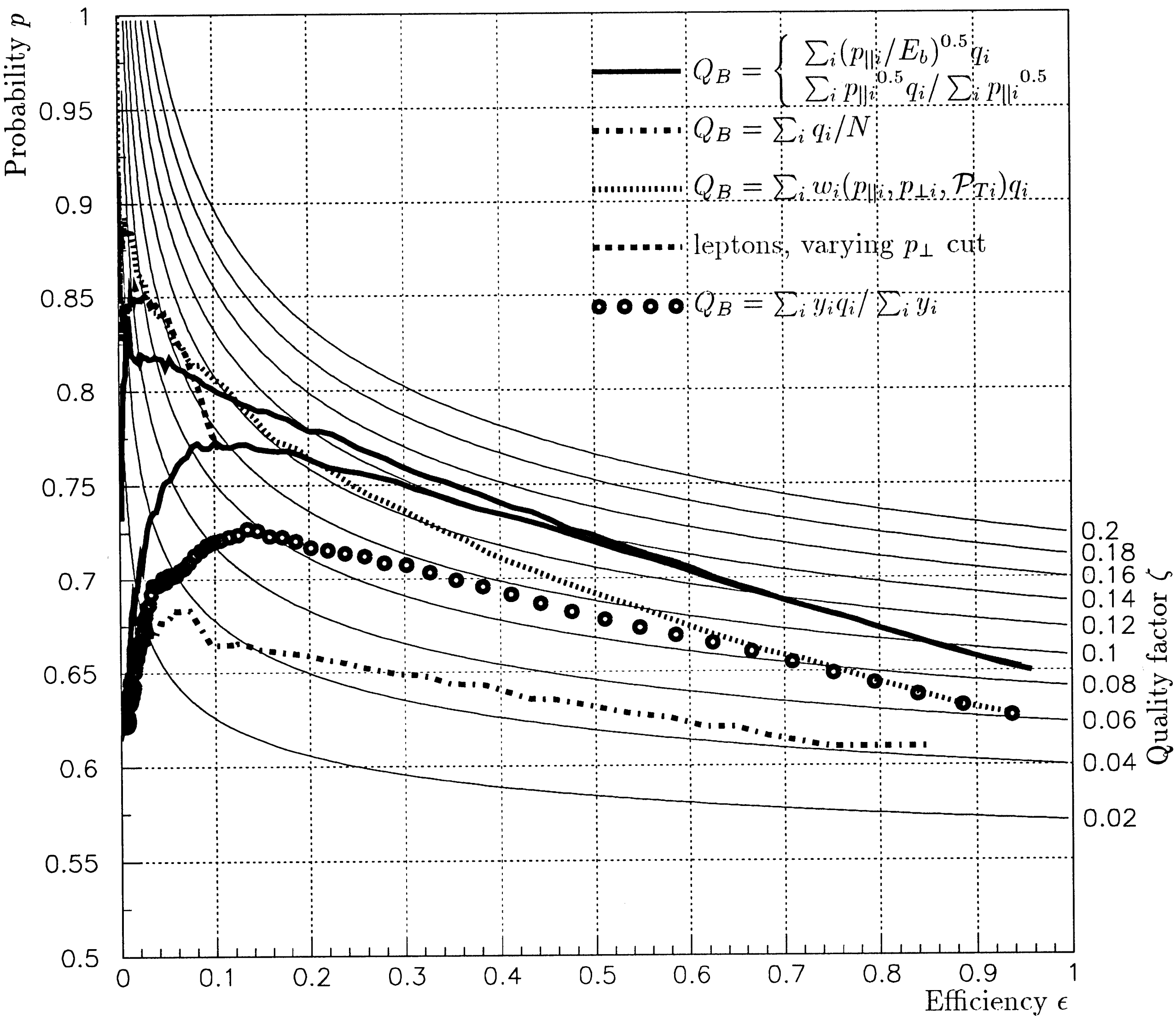

Figure 11: The probability p that a jet charge Q_B in the opposite hemisphere has the same sign charge as the b or $\bar{b}$ quark in that hemisphere, as it varies with the efficiency ϵ of the cut on $|Q_B|$. All Monte Carlo $Z \to b\bar{b}$ event hemispheres were used.

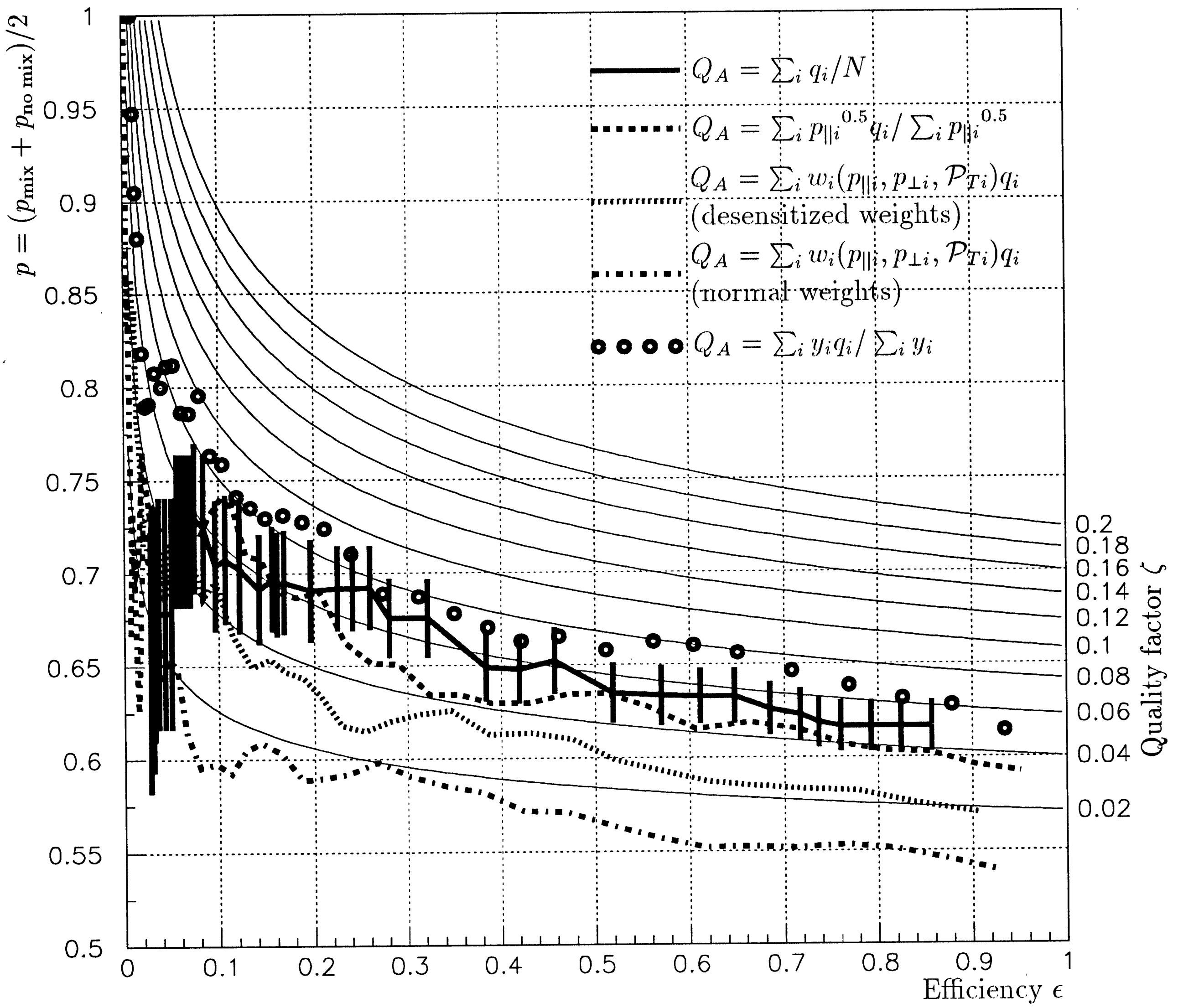

Figure 12: The mean probability $p = (p_{\rm mix} + p_{\rm no\ mix})/2$ in the same hemisphere, as it varies with the efficiency ϵ of the cut on $|Q_A|$, for different jet charges Q_A. The normal weights are those shown in Figure 6 and the desensitized weights are those shown in Figure 8. In order to simulate the situation in the same hemisphere, only those Monte Carlo $Z \to b\bar{b}$ hemispheres were used in which B_s^0 decayed to D_s^- or $\bar{B}_s^0$ decayed to D_s^+, and in which the $D_s^{\pm}$ was correctly reconstructed in the $\phi\pi$ decay channel. For clarity, error bars are only shown on one of the curves, and since a cut is being varied, these errors are correlated.

window $|m - m_{D_s}| < 10\,\mathrm{MeV}/c^2$. A special sample of 40 000 Monte Carlo $Z \to q\bar{q}$ events was used, generated such that the $\phi\pi$ decay sequence shown in Figure 3 occurred at least once per event[4]. The results of the fits are shown in Figure 13 for the ALEPH data 1991–1994, and in Figure 14 for the Monte Carlo.

Using the results of the fits and the values $c_A = 0.603$ and $c_B = 1.035$ calculated from Monte Carlo for the coefficients in (8), the efficiencies and probabilities for Q_{AB} were compared between data and Monte Carlo. The results are shown in Figure 15, and the data and Monte Carlo can be seen to be in good agreement.

7 Conclusions

A new jet charge method has been developed and its possible application in the setting of a lower limit for the B_s^0-$\bar{B}_s^0$ mixing parameter x_s has been discussed. For this analysis, a feature of the method was used to desensitize it to the tracks coming from the B_s^0 decay. This was done in order to reduce the systematic error coming from B decay model dependence. The weight functions prescribed by the method for use in the jet charge calculations were smooth and bounded just as for existing methods, creating no special systematic problems. Fits to the joint distribution of the jet charge in both event hemispheres showed good agreement between data and Monte Carlo for the performance of the method.

[4]The Monte Carlo sample was independent from the one used to calculate the weight function for Q_A

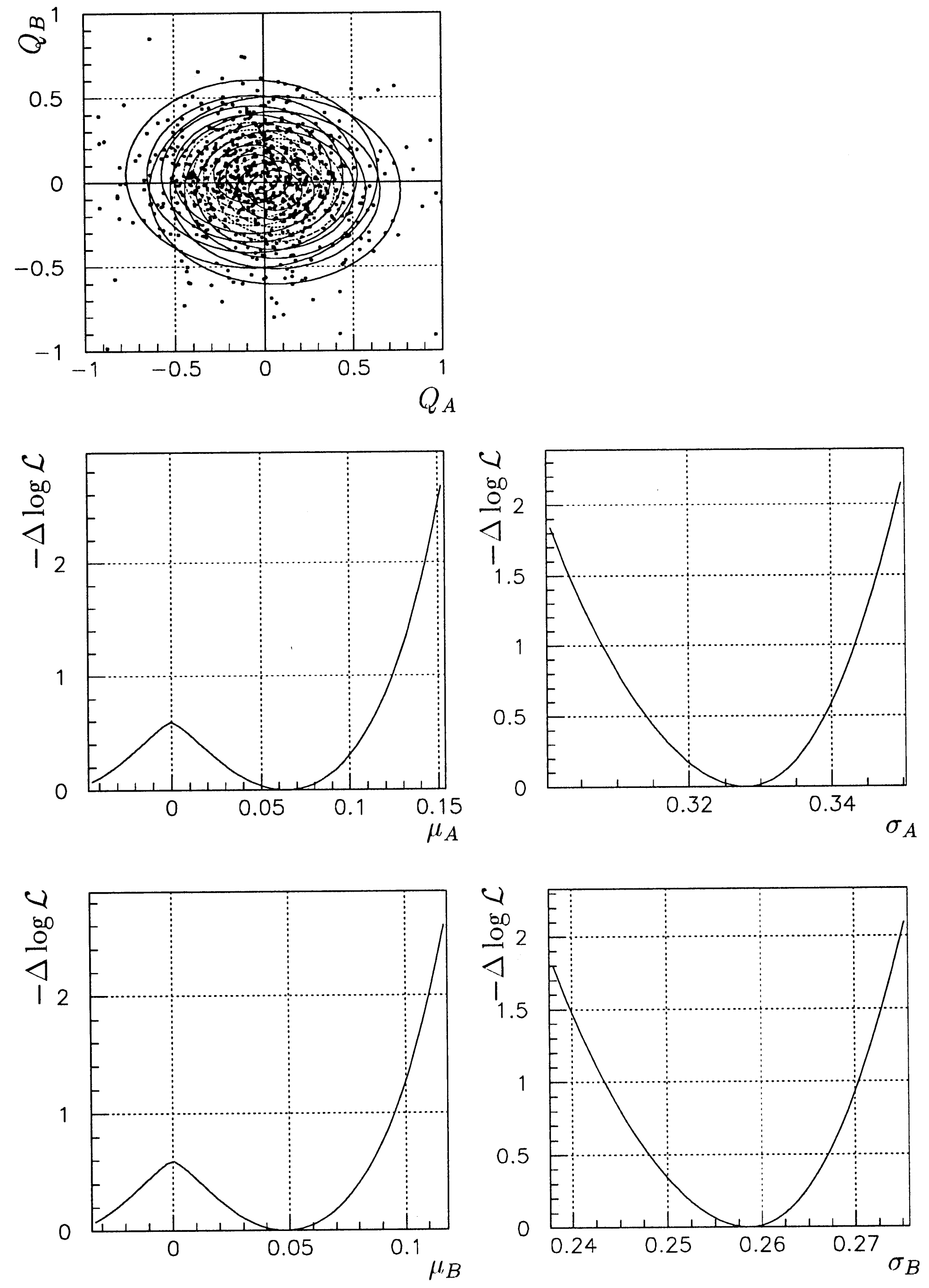

Figure 13: For the ALEPH data 1991-1994, the (Q_A, Q_B) distribution in events in which a $D_s^{\pm}$ candidate was reconstructed within the mass window $|m - m_{D_s}| < 10\,\mathrm{MeV}/c^2$, and the results of the unbinned log-likelihood fit to the distribution. The contours show the two Gaussian components of the function (27) after the fit, and the curves show the variation of $-\Delta \log \mathcal{L}$, the negative log-likelihood relative to the fitted minimum, when the individual parameters were varied about their fitted values and the remaining three parameters were refit at every point.

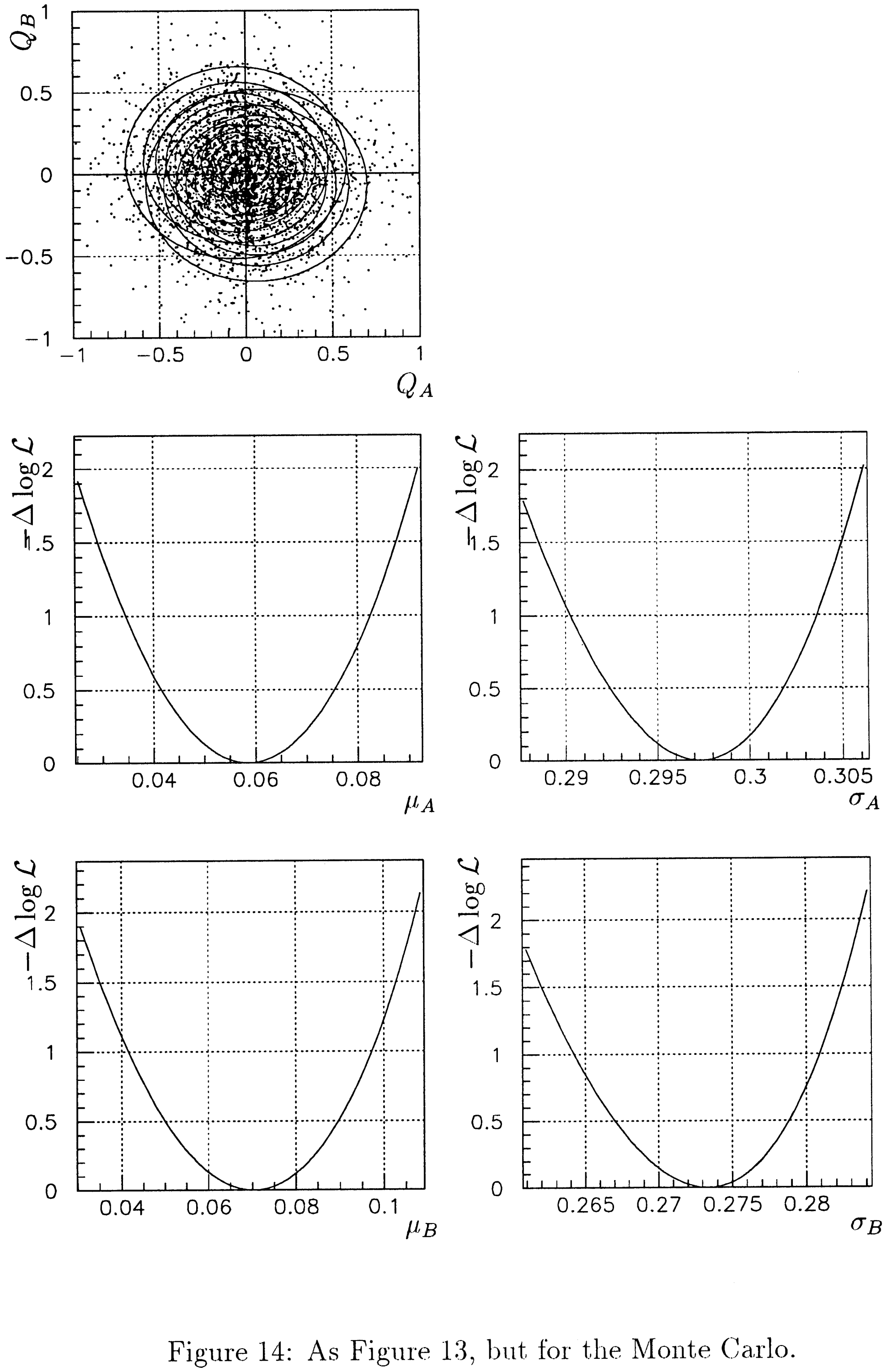

Figure 14: As Figure 13, but for the Monte Carlo.

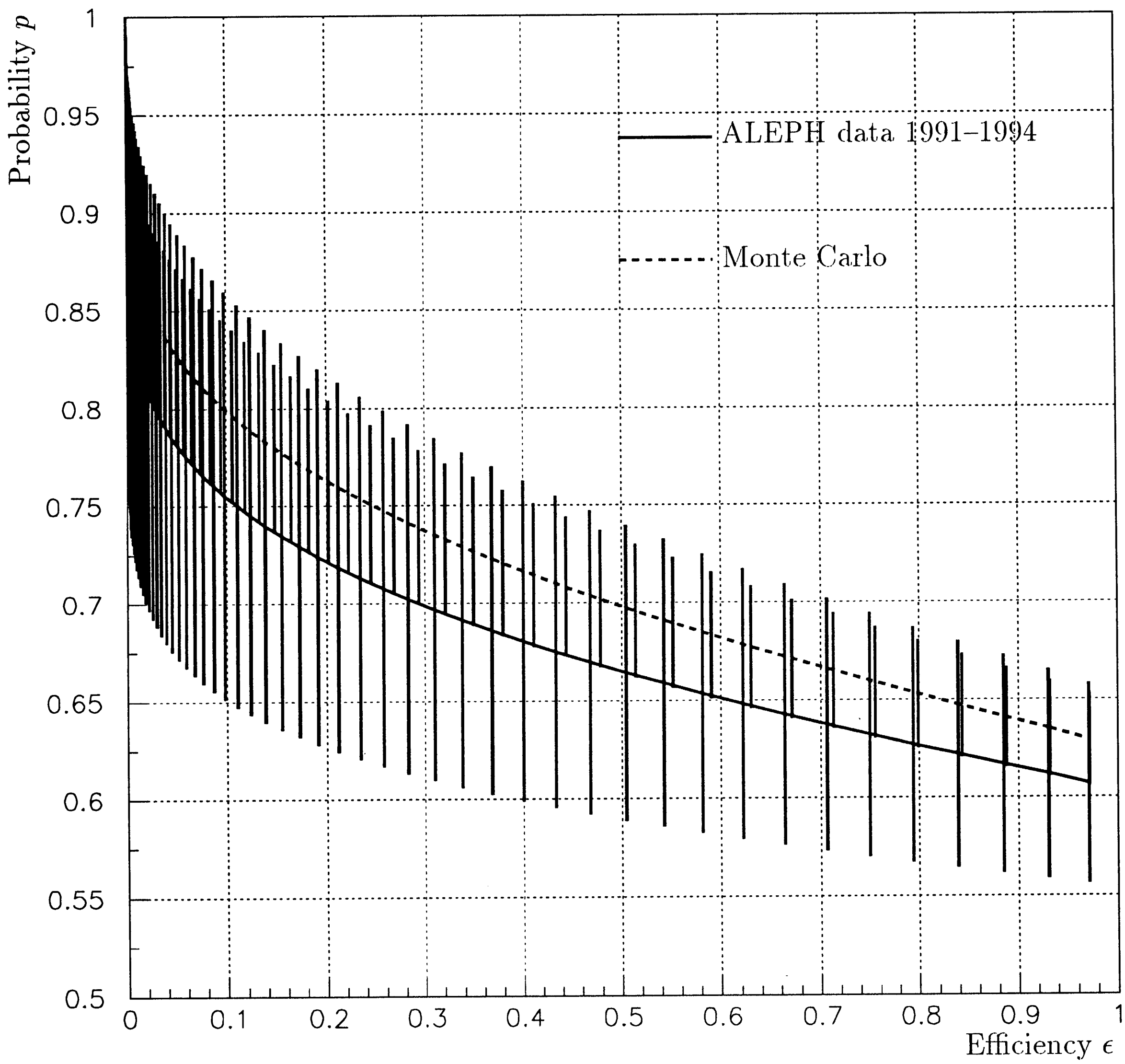

Figure 15: The probability p that the jet charge $Q_{AB} = 0.603Q_A - 1.035Q_B$ has the same sign charge as the b or $\bar{b}$ quark in the same hemisphere, as it varies with the efficiency ϵ of the cut on $|Q_{AB}|$, as determined by fits to the data and to the Monte Carlo.

References

[1] "Z Physics at LEP 1, Volume 3: Event Generators and Software", Edited by G Altarelli, R Kleiss and C Verzegnassi, CERN 89-08

[2] ALEPH Collab., D Buskulic et al, "Heavy Flavour Production and Decay with Prompt Leptons in the Aleph Detector", Z. Phys. C 62 (1994) 179-198

[3] OPAL Collab., R Akers et al, "Measurements of B^0-$\bar{B}^0$ mixing, $\Gamma(Z^0 \to b\bar{b})/\Gamma(Z^0 \to$ hadrons) and semileptonic branching ratios for b-flavoured hadrons in hadronic Z decays", Z. Phys. C 60 (1993) 199-216

[4] DELPHI Collab., P Abreu et al, "Measurement of the B^0-$\bar{B}^0$ mixing parameter in DELPHI", Phys. Lett. B 276 (1992) 379-392

[5] Particle Data Group, L Montanet et al, "Review of Particle Properties", Phys. Rev. D 50 (1994) 1173-1826

[6] R D Field and R P Feynman, "A Parameterization of the Properties of Quark Jets", Nucl. Phys. B 136 (1978) 1-76

[7] ALEPH Collab., D Decamp et al, "Measurement of Charge Asymmetry in Hadronic Z Decays", Phys. Lett. B 259 (1991) 377-388

[8] ALEPH Collab., D Decamp et al, "Measurement of B-$\bar{B}$ Mixing at the Z Using a Jet-Charge Method", Phys. Lett. B 284 (1992) 177-190

[9] ALEPH Collab., D Buskulic et al, "A Measurement of A^b_{FB} in Lifetime Tagged Heavy Flavour Z Decays", Phys. Lett. B 335 (1994) 99-108

[10] ALEPH Collab., D Buskulic et al, "Limit on B^0_s Oscillation Using a Jet Charge Method", CERN PPE 95-084

[11] OPAL Collab., P Acton et al, "A Measurement of the Forward-Backward Charge Asymmetry in Hadronic Decays of the Z^0", Phys. Lett. B 294 (1992) 436-450

[12] OPAL Collab., R Akers et al, "Measurement of the Time Dependence of $B^0_d \leftrightarrow \bar{B}^0_d$ Mixing Using a Jet Charge Technique", Phys. Lett. B 327 (1994) 411-424

[13] DELPHI Collab., P Abreu et al, "A Measurement of $\sin^2\theta_W$ from the Charge Asymmetry of Hadronic Events at the Z^0 Peak", Phys. Lett. B 277 (1992) 371-382

[14] DELPHI Collab., P Abreu et al, "Measurement of the B^0-$\bar{B}^0$ Mixing using the Average Electric Charge of Hadron-Jets in Z^0-Decays", CERN PPE 93-220

[15] H G Moser, "Minutes of the lifetime/mixing meeting 22-09-93. (Innsbruck)", ALEPH 93-156

[16] D Brown and M Frank, "Tagging b hadrons using track impact parameters", ALEPH 92-135

[17] See, for example, ALEPH on-line help with `HELP EDIR`